THE
PHYSICAL REVIEW

A journal of experimental and theoretical physics established by E. L. Nichols in 1893

SECOND SERIES, Vol. 138, No. 4A 17 MAY 1965

Measurement of Cesium and Rubidium Charge-Transfer Cross Sections*

JULIUS PEREL, RICHARD H. VERNON, AND HOWARD L. DALEY
Electro-Optical Systems, Inc., Pasadena, California
(Received 21 December 1964)

Charge-transfer cross sections for all cesium and rubidium ion-atom combinations were measured over energy ranges of 0.2 to 21 keV and 0.4 to 30 keV for the resonance and nonresonance combinations, respectively. A crossed-beam technique was used in which the atom beam was modulated by a mechanical chopper. Slow ions, produced by charge-transfer collisions, were extracted at the crossed-beam interaction region and detected using phase-sensitive lock-in techniques. Surface ionization was used to generate the ion beams and to detect the atom beams. The resonance cross sections are in general agreement with other experimental determinations and with theoretical predictions, except for the appearance of structure in our cross-section curves. The nonresonance cross sections show the expected adiabatic increase with velocity with the maximum near 10^{-14} cm^2 for Rb^+-Cs at a velocity of 23×10^6 cm/sec. The Cs^+-Rb maximum is also expected to occur at this velocity, which is just beyond the measured range. For each nonresonance cross section, four subsidiary peaks were observed below the velocity at the maximum. The two curves are similar in shape, with all of the Cs^+-Rb peaks occurring at the same velocities as the Rb^+-Cs peaks. The low-velocity portion of our Rb^+-Cs measurements is in good agreement with the data of Marino as regards the magnitude of the cross sections and the location of the first subsidiary peak. The cross-section curves of the four combinations are in very good agreement with the theoretical predictions of Rapp and Francis, particularly the ion velocity at the maximum for Rb^+-Cs. The subsidiary peaks appear to be related to electron transitions between the first excited states of the incident and product atoms. Incident-atom excited states are attributed to polarization excitation by the incident ion during the initial phases of the collision, and it is concluded that the atomic polarizability greatly affects the magnitude and shape of the cross-section curves.

INTRODUCTION

PAST theoretical and experimental investigations into charge-transfer collisions between ions and atoms have established the variation of the cross sections with the relative velocities.[1–3] The gross features of the cross-section velocity curves have been shown to be primarily determined by the energy defect (ΔE) given in the charge-transfer reaction

$$A^+ + B \rightarrow A + B^+ + \Delta E. \quad (1)$$

For resonance charge transfer in which $\Delta E=0$, the cross section (σ) exhibits a uniform decrease with the relative velocity (v) according to the relation

$$\sigma^{1/2} = a - b \ln v, \quad (2)$$

where a and b are constants for given ion and atom species. For the nonresonance case ($\Delta E\neq0$), the cross section increases uniformly with the velocity in the adiabatic region according to the relation

$$\sigma \sim \exp(-a|\Delta E|/vh), \quad (3)$$

where a is a length having atomic dimensions and h is Planck's constant. A cross-section maximum occurs at a velocity v_m which has been related to the absolute value of ΔE. Above v_m the cross section decreases according to Eq. (2).

In nonresonance charge transfer, if only electron transitions between the two ground states are considered, the cross-section velocity curves should increase monatonically to a single maximum with the velocity at the maximum related to the difference in ionization potentials. The inclusion of transitions between excited states should result in a superposition of cross-section curves with distributed structural peaks. The position and size of a given peak should depend upon the reaction-energy defect for that transition and the percentage

* This work was supported by the Independent Research and Development Program at Electro-Optical Systems, Inc.

[1] H. S. W. Massey and E. H. S. Burhop, *Electronic and Ionic Impact Phenomena* (Oxford University Press, New York, 1952).

[2] J. B. Hasted, *Advances in Electronics and Electron Physics* (Academic Press Inc., New York, 1960), Vol. 13.

[3] D. Rapp and W. E. Francis, J. Chem. Phys. **37**, 2631 (1962).

of the total number of charge-transfer collisions. Such structure observed in the past has been attributed to the presence of excited ions produced at the ion source.[4] However, the data of Marino[5] indicates the occurrence of a structural peak in the Rb^+-Cs charge-transfer cross sections with a surface ionization source which produces only ground-state ions. The preliminary report of our results[6] also indicated the presence of structure.

The Rb^+-Cs and Cs^+-Rb cross-section measurements reported in this paper show several subsidiary peaks which have been correlated with transitions between the first excited states of cesium and rubidium. The appearance of excited states are attributed to the induced polarization of the atoms by the colliding ions. Because of their large polarizabilities, alkali-metal atoms should exhibit large structural peaks in their cross section compared to other atoms. Structural peaks were also observed in the Cs^+-Cs and Rb^+-Rb cross sections. The present success in observing structure for resonance and nonresonance alkali-metal charge transfer is attributed to the small relative error in the measurements and the small interval between data points in the measured velocity range.

EXPERIMENTAL METHOD

In this investigation, a crossed-beam technique similar to that of Speiser and Vernon[7] was used to measure charge-transfer cross sections. A schematic diagram of the experiment is shown in Fig. 1. The ion beam was generated by a surface-ionization source and detected by a Faraday cup. The atom beam was formed by the collimation of an alkali-metal vapor effusing from a heated reservoir and detected by surface-ionization techniques. Slow ions, produced by charge-transfer collisions in the interaction region where the two beams crossed, were swept to a collector plate by an electric field across the interaction region. The atom beam was modulated by a chopping cylinder at a frequency of 30 cps to increase the signal-to-noise ratio, and the modulated slow-ion current was collected by the plate and amplified. This signal was frequency-selected and compared to a reference signal (produced by the atom-beam chopping system) at the lock-in amplifier. At a given ion-energy or ion-source accelerating voltage, three currents were measured as indicated in Fig. 1, and in addition the temperature of the atom-source exit aperture was measured. The charge-transfer cross section was calculated using these measured values. By varying the ion-source accelerating voltage, the absolute cross section was determined as a function of the ion velocity. For the ion-atom combinations and energy ranges of this investigation, the ion velocities were equivalent to the relative velocities to within 1%.

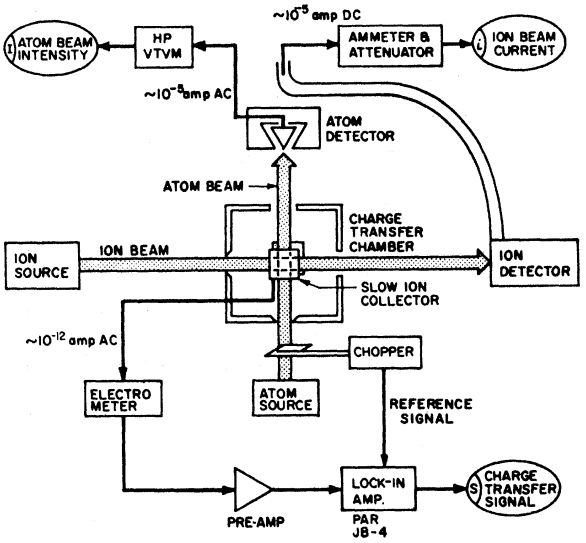

FIG. 1. Schematic diagram of the crossed-beam technique used in this experiment showing the signals measured.

Since total beam currents were measured using the crossed-beam technique, the charge-transfer cross section depends upon only one dimension of the interaction volume, the width of the widest beam. In this investigation, the atom-beam width was about three times that of the ion beam. This difference was sufficient to ensure that all of the ions passed through the atom beam even though the ion-beam width varied somewhat with the ion energy.

The charge-transfer cross section (in cm^2), in terms of the measurable parameters indicated in Fig. 1, is given by

$$\sigma = ev_a w(S/iI), \tag{4}$$

where e is the charge of the electron, v_a is the volocity of the atoms in cm/sec, w is the atom-beam width in cm, S is the charge-transfer signal in amperes, i is the total ion-beam current in amperes, and I is the total atom-beam intensity in amperes. The atom velocity is equal to the average velocity in the atom source[8,9] and is given by

$$v_a = (8kT/\pi m)^{1/2}, \tag{5}$$

where k is the Boltzmann constant, T is the temperature at the exit aperture of the atom source, and m is the mass of the atom.

DESCRIPTION OF APPARATUS AND TESTING

Ion Beam System

The ion source used in this investigation utilized surface ionization at a heated tungsten surface for the

[4] J. B. Hasted, in *Atomic and Molecular Processes*, edited by D. R. Bates (Academic Press Inc., New York, 1962) p. 696.
[5] L. L. Marino, in *Atomic Collision Processes*, edited by M. R. C. McDowell (John Wiley & Sons, Inc., New York, 1964) p. 807.
[6] J. Perel, R. H. Vernon, and H. L. Daley, Bull. Am. Phys. Soc. **9**, 536 (1964).
[7] R. C. Speiser and R. Vernon, American Rocket Society, No. 2068-61, New York, 1961 (unpublished).
[8] L. L. Marino, A. C. H. Smith, and E. Caplinger, Phys. Rev. **128**, 2243 (1962).
[9] J. Perel, P. Englander, and B. Bederson, Phys. Rev. **128**, 1148 (1962).

generation of ions. This type of single-beam alkali-metal source has been extensively used at this laboratory for supporting research associated with ion propulsion programs.[10] The surface ionizer was composed of a single porous tungsten button which had a density approximately 80% that of solid tungsten. Alkali-metal vapor supplied from a reservoir to the rear of the tungsten at a pressure of a few Torr diffused through the porous tungsten to the front surface where ions were formed. An accel-decel electrode configuration produced an electric field which extracted and accelerated the ions; two sets of deflection plates were used to position the ion beam at the charge-transfer chamber. The ion beam was detected by a Faraday cup which had a 5:1 depth-to-aperture ratio, and which was operated at a positive potential to suppress secondary electrons.

The ion source was operated at acceleration voltages of 0.2 to 30 kV for both cesium and rubidium. Total ion currents of greater than 1 mA for both cesium and rubidium were extracted from the source at accelerating voltages greater than 2 kV, with no essential difference in source performance using cesium or rubidium.

The ions were formed at a well-defined surface by surface ionization and were uniformly accelerated to the desired velocity by a large electric field. All ions were emitted from an equipotential surface and had an energy spread initially determined by the ionizer temperature. The ions in the beam had a somewhat greater energy spread due to the beam potential distribution. This was estimated to be below the 1% precision of the voltmeter used to calibrate the accelerating voltage power supplies.

Atom-Beam System

The atom source was a stainless steel reservoir with a circular exit aperture of 0.1-cm diam. Alkali-metal vapor flow, which determined the atom-beam intensity, was controlled by a valve and the reservoir temperature. Iron-constantan thermocouples were used to measure the temperature at the exit aperture. The atom beam was modulated at a rate of 30 cps by a chopping cylinder, producing a trapezoidal waveshape. Detection of the atom beam was accomplished utilizing surface ionization on a large-area tungsten filament heated indirectly by a resistance heater. Ions leaving the ionizing surface were accelerated by an electric field to a grounded collector and the current was measured by an ac vacuum-tube voltmeter. The collector was cooled with liquid nitrogen to prevent re-evaporation of the collected alkali atoms.

A series of tests were performed to examine the characteristics of the atom source and of the atom detector, for both cesium and rubidium. Included were atom-detection-current measurements as a function of the ionizer temperature and collection voltage to ensure that the atom detector was always operated in the ion emission limited region.

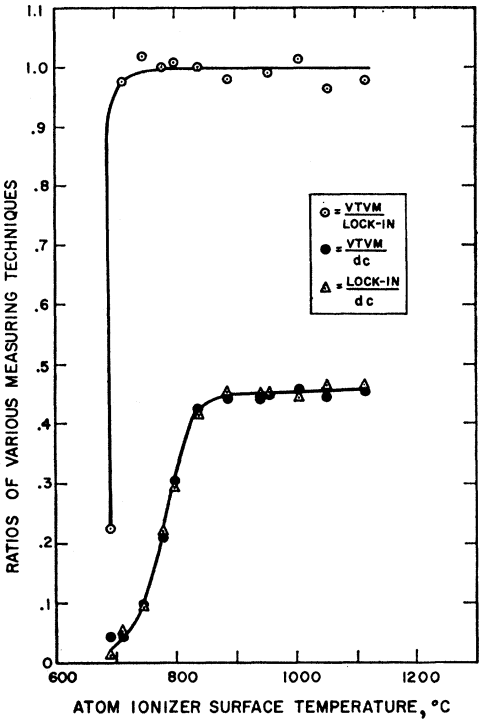

FIG. 2. Ratios of trapezoidal signals using various measuring techniques. The input signals were obtained from the detector of the modulated rubidium atom beam for different surface-ionizer temperatures. The upper curve, representing the ratio of the vacuum-tube voltmeter to the lock-in readings, shows the calibration factor for the S/I term in Eq. (4) to be unity. The flat portion of the lower curve defines the operating-ionizer temperature range and shows that the rms value of the fundamental component and the rms value of the wave are both 0.45 of the peak-to-peak amplitude for this trapezoidal wave.

The atom beams were operated in two modes, a dc mode and a modulated or ac mode. Atom-beam-detection signal measurements were performed at various ionizing surface temperatures using the lock-in amplifier, the VTVM and the dc microvolt-ammeter in rapid sequence. The measurements were compared to determine the atom-beam detector characteristics and to calibrate the atom ac detection system and the charge-transfer detection system. The ratios of the various measurements over a wide temperature range are shown for rubidium in Fig. 2. The upper curve is the ratio of the VTVM to the lock-in readings. The flat portion of the curve is a measure of the calibration factor for the cross-section determinations: The charge-transfer signal was measured by the lock-in amplifier which determines the rms value of the fundamental component, while the atom-beam intensity was measured by the VTVM which determines the rms value of the trapezoidal wave. The measured cross section is proportional to the ratio of these two signals and requires a calibration factor. This factor was determined to be unity, both experimentally and analytically from wave

[10] G. Kuskevics and B. Thompson, AIAA J. 2, 284 (1964).

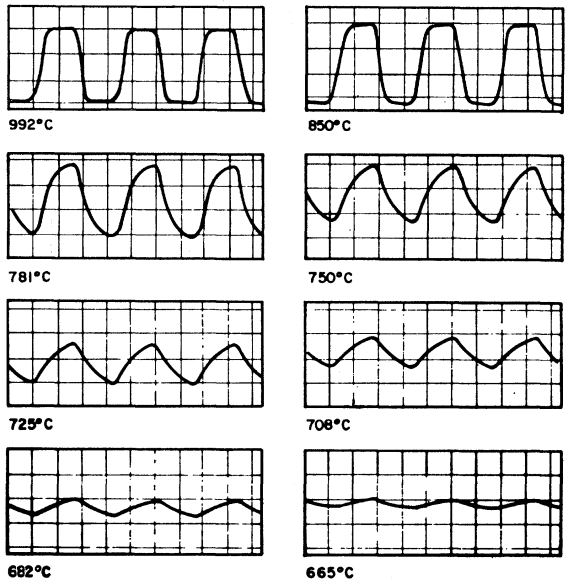

FIG. 3. Cesium atom-beam detection-signal wave shape as a function of ionizing surface temperature from oscilloscope photos (vertical scale, 5μA/division; horizontal scale, 10 msec/division). Note the amplitude attenuation and phase shift with decreasing temperatures below 850°C, due to the increasing desorption time for ion emission.

shape considerations. The lower curve in Fig. 2 represents the ratios of the VTVM and lock-in readings to the dc readings for rubidium. The flat portion of this curve determines the operating temperature range of the atom-beam surface ionizer and that fraction of the dc atom-beam detected by the ac instruments. The ratio 0.45 was used to compute a wave shape which agrees with the atom-beam wave shape. The sloping portion of the curve shows the effect of the wave distortion on the ac determinations.

The distortion of the atom-beam wave-shape signal as the desorption time increases (i.e., as the ionizing surface temperature decreases) is illustrated in Fig. 3. To ensure proper detection-system operation the desorption times for the emission of cesium and rubidium ions from tungsten were measured using ac modulation techniques.[9,11] The results, in good agreement with those of other investigators, clearly defined the minimum temperature for distortion-free operation of the detector.

A measurement was made of the attenuation of the atom beam by residual gas molecules over a pressure range from 1×10^{-6} to 5×10^{-5} Torr. The beam intensity showed an exponential variation with pressure with only a 2% beam loss at 1×10^{-6} Torr (the highest operating pressure during cross-section measurements). Because of the large acceptance angle of the detector, there was no discrimination against small-angle scattering and, as a result, the scattering cross-section determination was a factor of 3 below reported values for $Cs\text{-}N_2$.[12]

Charge-Transfer Detection System

The ion and atom beams crossed at right angles to each other within the liquid-nitrogen-cooled charge-transfer chamber. The slow-ion or charge-transfer collector plates were in planes parallel to both the ion and atom beams and had areas that were larger than the projected area of the intersecting beams. These plates were provided with potential guard plates to minimize fringing of the electric field that crossed both beams. A small dc potential was applied between the plates to extract the slow ions formed in charge-transfer collisions.

An electrometer was used to convert the charge-transfer signal from a current signal to a voltage signal. The voltage signal was amplified by a low-noise preamplifier and a narrow-band amplifier tuned to the modulation frequency (30 cps), and then phase-compared to a reference signal of the same frequency. This reference signal was mechanically generated by a light source, a photocell, and a second chopping cylinder which utilized the rotating shaft it shared in common with the atom-beam chopper.

Periodic tests were made to assure reliable operation of the charge-transfer detection system. The tests included linearity determinations of the cross-section equation [Eq. (4)]. At a given ion energy and atom-source temperature, the ratio S/iI should remain constant and therefore linearity of the detection system could be determined by varying the ion beam and the atom beam independently. The results of these tests showed that changes in the atom-beam intensity and the ion current did not appreciably affect the ratio.

In addition to linearity checks, the charge-transfer signal was measured as a function of the voltage across the slow-ion collector plates. The results indicated a space-charge limited rise to a maximum with a slight decrease in signal strength as a collection voltage was increased. The decreased signal strength with increasing voltage was attributed to leakage currents. The collection voltage selected was sufficiently high to be out of the space-charge limiting region, but low enough to reduce leakage currents to values that would not change the electrometer tube characteristics.

The charge-transfer signal was in the range of 10^{-12}- to 10^{-10}-A rms. This signal range had a very favorable signal-to-noise ratio, as illustrated in Fig. 4, in which the signal wave shape under optimized conditions closely resembled the atom-beam wave shape. Ion-source sparking, ion-beam fluctuations, and decreases in the ion-beam current reduced the signal-to-noise ratio in certain energy regions. This reduction affected the accuracy of the cross-section determinations primarily at energies below 0.5 and above 20 keV.

[11] J. Perel, R. H. Vernon, and H. L. Daley, J. Appl. Phys. (to be published).

[12] I. Estermann, S. M. Foner, and O. Stern, Phys. Rev. **71**, 250, (1947).

DATA REDUCTION AND ERROR

A data run consisted of measuring the experimental parameters given in Eq. (4) from one end of the ion velocity range to the other, with the succeeding run made in the reverse direction. Several runs were made for each of the four ion-atom combinations at a variety of ion-beam currents and atom-beam intensities. Each run displayed the curve shape and structure consistent with the final averaged data, but the absolute cross-section values varied from run to run producing a typical spread in the data points of about 15%. When the separate runs were normalized to the average curve, the data spread was sharply reduced, yielding a much higher accuracy for the relative curve shape.

The relative curve shape for Rb^+-Cs is illustrated in Fig. 5; a single continuous run (of several minutes duration at constant atom-beam intensity) is reproduced from a strip-chart recording. For this run the ion-beam energy was continuously varied while the charge-transfer signal and the ion-beam current were recorded. In the energy range in which the ion-beam current remained constant, the curve shape is essentially the same as the curve obtained from the average values of discrete measurements.

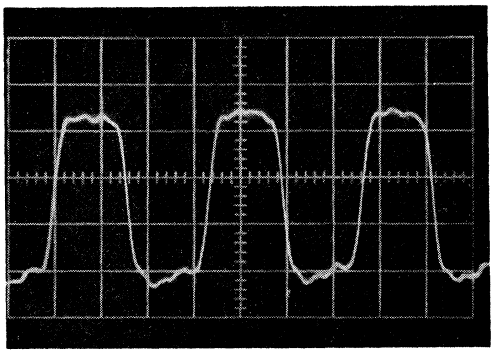

(a)

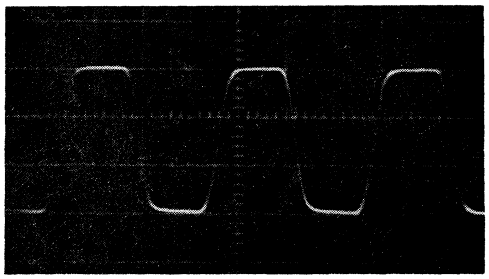

(b)

FIG. 4. Comparison of charge-transfer signal and atom-beam wave shapes from oscilloscope photos. Note the very favorable signal-to-noise ratio seen in the charge-transfer signal (peak-to-peak current of about 1.5×10^{-10} A). (a) Charge-transfer signal: Rb^+-Rb at 10 kV; vertical scale $=5\times10^{-11}$ A/div; horizontal scale = 10 ms/div. (b) Atom beam: Cs beam; ionizer temperature 992°C; vertical scale $=5\times10^{-6}$ A/div; horizontal scale = 10 ms/div.

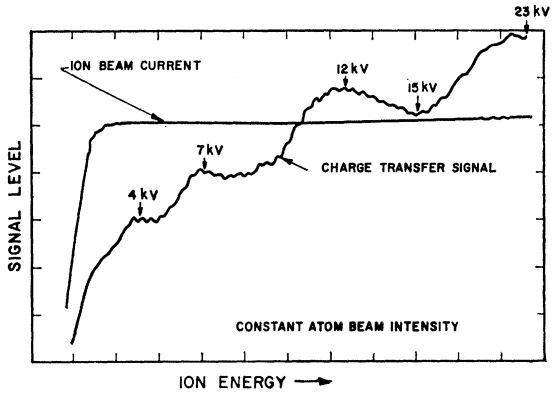

FIG. 5. Rb^+-Cs charge-transfer curve shape from a strip-chart recorder trace. The ion-beam energy was varied continuously for a time interval of several minutes. In the range that the ion current remained constant, the curve shape shows good agreement with Fig. 8.

The dependence of the charge-transfer signal on the critical interaction dimension in Eq. (4) (i.e., the width of the widest beam) was examined for two different beam-interaction arrangements. With the ion-beam width the critical dimension, a varying systematic error resulted which was attributed to changes in the ion-beam width at different ion energies. This error was eliminated when the atom beam was made the widest beam; although the atom-beam width was somewhat uncertain, it did not vary with the ion energy. All the reported data were acquired with this arrangement since it resulted in a much higher relative accuracy. The atom-beam width was computed to be 0.39 cm with an uncertainty of $\pm7\%$. This uncertainty was comparable to the spread in the unnormalized data points and was the dominant factor in the accuracy of the absolute-cross-section determinations.

Contributions to the charge-transfer signal by ionization collisions were negligible since the collector system discriminated against all but unpaired charges arriving at the modulation frequency. In addition, when a different collector arrangement was used, ionization collision signals were observed to be below 2% of the charge-transfer signal for Rb^+-Rb at 10 keV. Erroneous signals produced by large-angle elastic scattering of ions at the modulation frequency were also negligible, since cross sections for large-angle scattering are believed to be at least 2 orders of magnitude below charge-transfer cross sections. The total error in the charge-transfer signal estimated at the precision of the electronics was about 4%.

The errors ascribed to the relative curve shapes over most of the velocity range were typically $\pm3\%$ for the four resonance and nonresonance cross-section determinations. This error was larger at each end of the velocity range for all but the cesium resonance case. The overall error in the absolute values for all four cross-section determinations was estimated at $\pm8\%$.

RESULTS AND ANALYSIS

Resonance and nonresonance charge transfer cross-section velocity curves are presented for the four cesium-rubidium ion-atom combinations and compared with the results of other investigators. The resonance and nonresonance combinations are then compared to one another to illustrate features they have in common. These features are correlated with a qualitative model in an effort to determine those atomic and collisional parameters of significance in charge-transfer interactions.

Resonance Charge Transfer

The resonance cross sections of Cs^+-Cs and Rb^+-Rb are shown in Figs. 6 and 7, respectively. The results show general agreement in magnitude with most of the experimental curves but show a less rapid decrease with velocity, which is in better agreement with a theoretical curve based on Firsov's method[13] (curve F). The results of Chkuaceli *et al.*[14,15] were reduced[16] by 15% because they used average atom-beam velocities rather than average velocities in the atom source for their determinations. The Cs^+-Cs results of Kushnir and Buchma[17] show good agreement with our data. Also, several subsidiary peaks were observed in our cross-section curves giving structure not previously

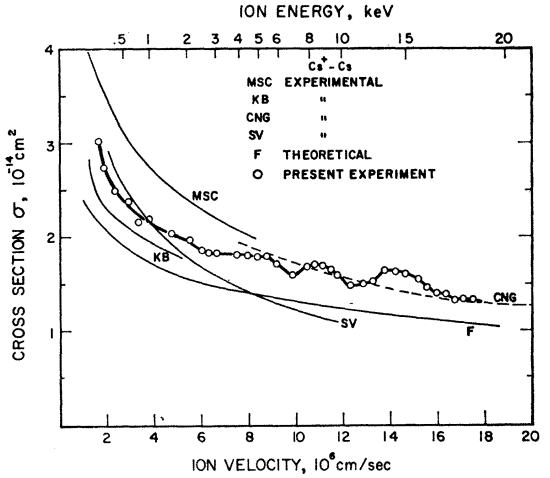

FIG. 6. Cs^+-Cs charge-transfer cross section versus ion velocity. Other results are included for comparative purposes: MSC—Marino, Smith, and Caplinger (Ref. 8); KB—Kushnir and Buchma (Ref. 17); CNG—Chkuaceli, Nikoleychvili, and Gouldamachvili (Ref. 14); SV—Speiser and Vernon (Ref. 7); F—theoretical curve based on Firsov's method (Ref. 13).

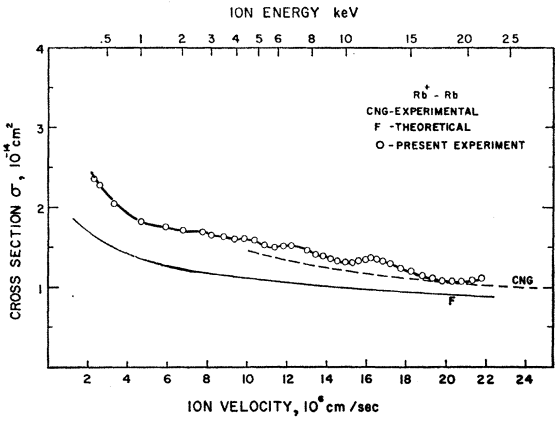

FIG. 7. Rb^+-Rb charge-transfer cross section versus ion velocity. Other results are included for comparative purposes: CNG—Chkuaceli, Nikoleychvili, and Gouldamachvili (Ref. 14); F—theoretical curve based on Firsov's method (Ref. 13).

reported. Several investigators show data points lying off the smooth curve in approximate coincidence with the structure in our resonance curves.

Our resonance data in general varies with the ion velocity in accordance with Eq. (2). Nominal values of the constants as determined from the data are $a=42\times10^{-8}$ cm and $b=1.85\times10^{-8}$ cm. The constants are slightly different for cesium and rubidium, although the presence of structure in the curves prevented sufficiently precise determinations of the difference.

A low-accuracy determination of the Rb^+-Rb cross section was made at 12.3 keV by measuring the charge-transfer signal using dc techniques. This dc determination of 1.6×10^{-14} cm² was in close agreement with the averaged ac result of 1.4×10^{-14} cm².

Nonresonance Charge Transfer

The cross section for charge transfer between ions and atoms of unlike species increases with increasing energy in the low-energy adiabatic region. At the termination of this region the cross section reaches a maximum, then decreases with increasing energy. Most of the measurements on alkali-metal nonresonance combinations made prior to our investigation were limited to the adiabatic region and include Rb^+-Cs by Marino[5] using the beam through a vapor technique; and Rb^+-Cs, K^+-Cs, Na^+-Cs, Cs^+-Rb, Cs^+-K, and Cs^+-Na by Chkuaceli *et al.*[15] using the crossed-beam technique.

Figure 8 shows the Rb^+-Cs experimental results and those of Marino and Chkuaceli *et al.* The agreement between our curve and that of Marino is very good, particularly in the position and shape of the first peak. However, Marino's results do not show the presence of the second peak. There is also good agreement in the absolute magnitude since the error ranges overlap in the velocity range common to both curves. With or without the correction of the results of Chkuaceli

[13] O. B. Firsov, Zh. Eksperim. i Teor. Fiz. 21, 1001 (1951).
[14] D. Chkuaceli, U. D. Nikoleychvili, and A. I. Gouldamachvili, Bull. Acad. Sci., USSR 24, 972 (1960).
[15] D. Chkuaceli (Tchkouaceli), A. I. Gouldamachvili, and U. D. Nikoleychvili, *Sixth International Conference on the Ionization Phenomena of Gases* (S.E.R.M.A., Paris, 1963), pp. 475–479.
[16] N. F. Ramsey, *Molecular Beams* (Oxford University Press, New York, 1956).
[17] R. Kushnir and I. Buchma, Bull. Acad. Sci., USSR 24, 989 (1960).

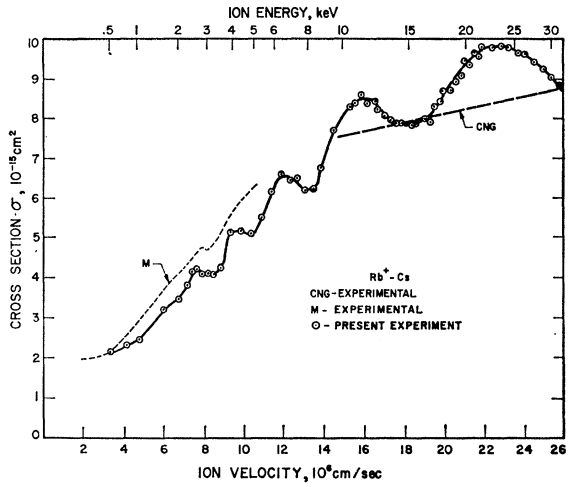

FIG. 8. Rb^+-Cs charge-transfer cross section versus ion velocity and energy. Curve M, the results of Marino (Ref. 5), compares very favorably with the present results, particularly in the position of the first subsidiary peak. Curve CNG, the corrected results of Chkuaceli, Gouldamachvili, and Nikoleychvili (Ref. 15), is in general agreement with our cross sections.

et al., their cross-section values are in general agreement with our data. Their quoted reproducibility of $\pm 16\%$, coupled with the measurement of only five data points, precluded the observation of curve structure. The structure observed in our Rb^+-Cs cross-section curve showed a total of five peaks. It is felt that the fifth peak is the cross-section maximum which terminates the adiabatic region, because the appearance of an additional broader and higher peak could make the cross section larger than the Cs^+-Cs cross section at that velocity, which is unlikely.

The results of the Cs^+-Rb cross-section determinations are shown in Fig. 9. The corrected results of Chkuaceli *et al.* are also shown, but the agreement is not as good as the Rb^+-Cs case. Our experimental curve shows only four peaks although a fifth, lying out of the measured energy range, is implied from the similarity to the Rb^+-Cs results. Both of our nonresonance curves are similar in that they have structure and in general show the adiabatic increase with velocity in accordance with Eq. (3).

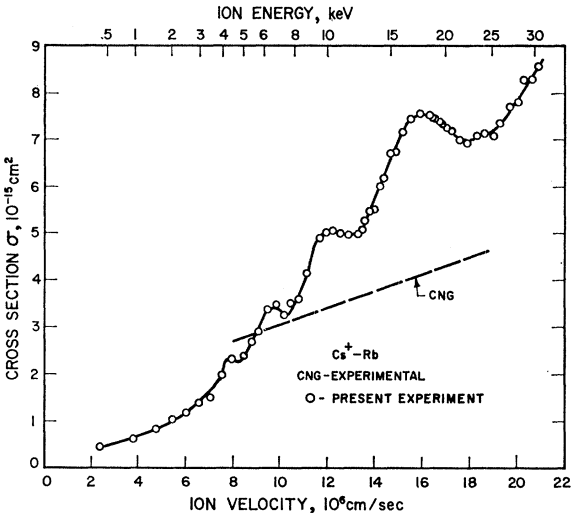

FIG. 9. Cs^+-Rb charge-transfer cross section versus ion velocity and energy. Curve CNG, the corrected results of Chkuaceli, Gouldamachvili, and Nikoleychvili (Ref. 15), was constructed from five data points.

Comparison of Resonance and Nonresonance Structure

Figure 10 shows our experimental cross sections as a function of ion velocity and Table I contains a listing of the ion velocity at each of the peaks. The peaks in the cesium resonance curve are uniformly displaced from those in the rubidium resonance curve and are more pronounced. The four subsidiary peaks for both nonresonance curves occur at the same ion velocities,

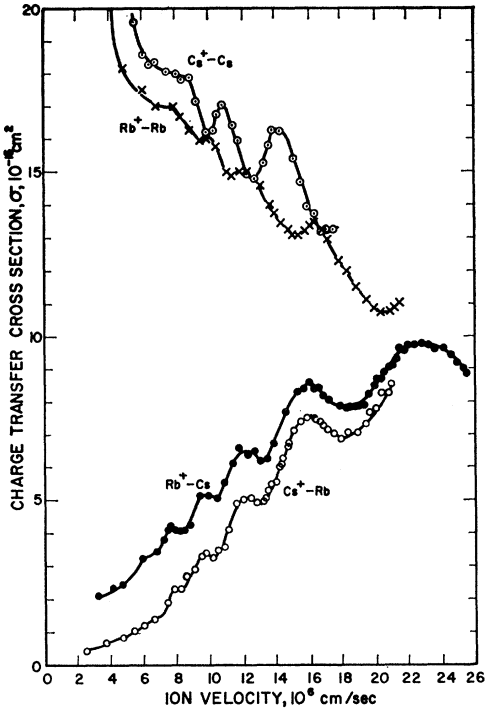

FIG. 10. Cesium and rubidium charge-transfer cross section versus ion velocity. The comparative positions and amplitudes of the structural peaks are illustrated.

TABLE I. Ion velocity (10^6 cm/sec) at each of the peaks.

Cs^+-Cs	Rb^+-Rb	Cs^+-Rb	Rb^+-Cs
8.7	7.6	7.8	7.7
10.8	9.9	9.7	9.7
14.0	12.3	12.1	12.0
	16.3	16.0	16.2
			23.0

with the Rb^+-Cs peaks somewhat more pronounced than those of Cs^+-Rb. The more pronounced peaks in the resonance and nonresonance curves appear to be associated with cesium being the incident atom. A further examination of the two nonresonance curves indicates that the fifth Cs^+-Rb peak could readily occur at the same velocity as the Rb^+-Cs maximum. The cross-section curves are widely separated at low velocities and approach each other with increasing velocities while the size of the peaks increases with increasing velocities.

Theoretical Consideration and Comparison of the Results

The charge-transfer cross sections for all four cesium and rubidium ion-atom combinations were compared to examine their agreement with the predictions of Hasted[2] and those of Rapp and Francis[3] and to determine the possible causes of the curve structure. The theoretical models are based upon a two-state approximation; that is, only the ground states of the incident and the product particles are included. Thus, the prediction of the velocity at the cross-section maximum depends only upon the energy difference between these two ground states. The inclusion of excited states for the incident and product particles could result in several peaks, each depending upon the particular energy differences between the states.

From the nonresonance results it is clear that the maxima are at velocities much greater than the 5×10^6 cm/sec predicted by Hasted's adiabatic maximum rule. An "effective" polarization energy correction proposed by Hasted[18] was calculated but only shifted the predicted maxima to a velocity of 8×10^6 cm/sec. The magnitude of this polarizability effect was not sufficient to explain the observed phenomena for the nonresonance cesium-rubidium ion-atom combinations. An attempt was made to correlate the nonresonance subsidiary peaks with the adiabatic maximum rule by assuming multistate transitions between the ground state and first excited states of both cesium and rubidium. Since no general correlation was found, it was concluded that a strict application of this rule is not valid for these ion-atom combinations and is possibly invalid for all alkali-metal combinations.

Figure 11 shows monotonic approximations of the results on a semilog plot. The RF curves represent the theoretical predictions of Rapp and Francis[3] for Cs^+-Cs and a cesium nonresonance curve for $\Delta E=0.3$ which closely corresponds to the cesium-rubidium ground state energy defect. The over-all agreement in curve shapes is extremely good and the location of the theoretical resonance curve below the experimental data is consistent with most experimental-theoretical comparisons cited by Rapp and Francis. The nonresonance maximum predicted at about 22×10^6 cm/sec is very close to the experimental maximum, about 23×10^6 cm/sec.

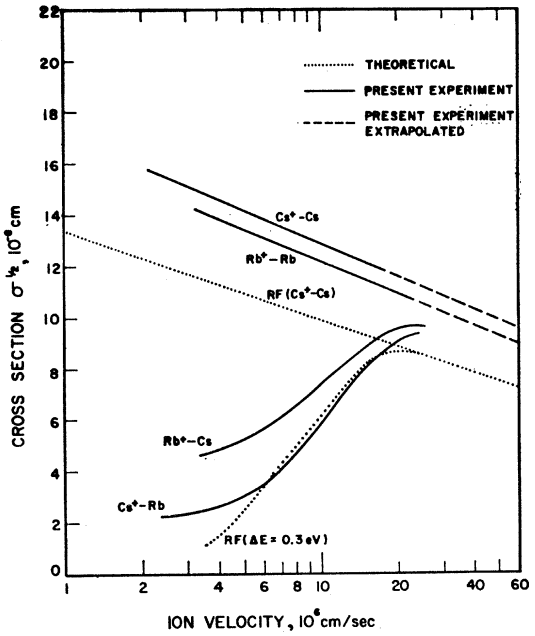

FIG. 11. Charge-transfer cross-section results versus ion velocity compared with the theoretical curves RF of Rapp and Francis (Ref. 3). Our results are shown as a monotonic approximation of the experimental data to eliminate the detailed structure.

Motivated by the good agreement between the maximum predicted by Rapp and Francis and the experimental results, the positions and relationships of the experimental peaks of all four cesium and rubidium combinations were examined for correspondence with these predictions by including multistate transitions. By assuming that the energy difference between any two energy states determines the velocity at the cross-section subsidiary peak, multistate transitions between the two $6P$ states of cesium and the two $5P$ states of rubidium were examined for correspondence with the subsidiary peaks. Table II contains the energy differences between each of the first excited states, matched

TABLE II. Velocity comparison of computed and experimental peaks.

Transition	ΔE[a] (eV)	Computed peaks (based on ref. 3) Velocity (10^6 cm/sec)	Experimental peaks velocity (10^6 cm/sec)
Cs($6^2P_{1/2}$)-Rb($5^2P_{3/2}$)	0.080	8	7.7– 7.8
Cs($6^2P_{1/2}$)-Rb($5^2P_{1/2}$)	0.110	10	9.7
Cs($6^2P_{3/2}$)-Rb($5^2P_{3/2}$)	0.149	13	12.0–12.1
Cs($6^2P_{3/2}$)-Rb($5^2P_{1/2}$)	0.178	15	16.0–16.2
Cs($6^2S_{1/2}$)-Rb($5^2S_{1/2}$)	0.283	22	23

[a] The energy differences were taken from C. E. Moore, *Atomic Energy Levels* (National Bureau of Standards, Washington, D. C., 1958), Vol. II (1952)-Rb, Vol. III (1958)-Cs, NBS-467.

[18] J. B. Hasted and A. R. Lee, Proc. Phys. Soc. (London) **79**, 702 (1962).

with the corresponding velocity based on Rapp and Francis and compared with the velocity at the experimental peaks. The computed peaks are in very good agreement with the experiment peaks, although distributed over a smaller velocity range.

Although thermal-alkali-atom beams are essentially free of excited states, multistate transitions are possible if excitations of the incident atoms are induced by the initial interaction with the incident ion. Polarization mixing of S and P states may, in effect, produce excited states. This "polarization excitation" should principally affect alkali-metal atoms since they have the highest polarizabilities of all the elements. The mechanism is essentially the same as the coupling of the ground S state and the first excited ^2P states used to explain the cross-section peak for low-energy electron alkali-metal atom scattering.[19] Only one peak appears in the electron-scattering case because the ^2P states have a small energy separation compared to the energy difference between these states and the ground state. The four subsidiary peaks in charge transfer are attributed to transitions between the two levels of the first excited state of cesium and the two levels of the first excited state of rubidium. For these atoms the two levels of the first excited states have a sufficient energy separation to produce distinguishable peaks in the measured ion velocity range.

When only first excited states are considered, this simple "polarization excitation" approach does not explain the presence of more than one subsidiary peak for the resonance cases in the velocity range of this experiment. The polarization mixing of S and P states may instead produce virtual states that are different from the energy states of the free atom. The effective states or the states of a quasimolecular ion formed during the collision can, in turn, alter the effective values of the energy defects. Alterations of the free-atom energy defects could cause the shifting of the subsidiary peaks in the nonresonance cases and explain the presence of more than one peak in the resonance cases.

If it is assumed that excitation occurs in the initial stages of the collision, de-excitation may occur in the final stages of the collision or the product atoms may leave the collision interaction in an excited state and subsequently emit a photon. The detection of the characteristic radiation from the product atoms could correlate the cross-section peaks with particular energy-level transitions. In general this model indicates that polarization could be the mechanism for energy transformations between potential energy (i.e., the energy defect) and kinetic energy for nonresonance charge transfer.

It appears that the values of the cross section depend upon the incident atom parameters rather than those of the incident ion as formulated by Rapp and Francis. In examining the results of Allison[20] for helium ions and inert-gas atoms, it is found that the value of the cross section at the maximum increases with increasing energy defect (in going from neon to xenon). This is in direct contrast with the Rapp and Francis model in which the cross section at the maximum for a given ion decreases with increasing energy defect, since they relate the nonresonance cross sections with the ion resonance curve. If each of these nonresonance cross sections is associated with the resonance curve of the incident atom, better agreement between theory and experiment is attained.

On the basis of the above considerations, the Rb^+-Cs charge-transfer cross section at the maximum should exceed that of Cs^+-Rb. Furthermore, in predicting cross sections for interchanged ion-atom species of the rest of the alkali-metal combinations, the ratios should depend upon the ratios of the incident-atom polarizabilities in addition to the energy defects. For example, since the polarizability of potassium is only somewhat smaller than that of rubidium, the values of the K-Rb cross sections at the maxima should not differ greatly for interchanged ion-atom species, but should exceed the Rb^+-Cs and Cs^+-Rb cross sections. Based on the correlation between the results of this experiment and the theoretical model of Rapp and Francis, these maxima should occur at a velocity of about 15×10^6 cm/sec, with the location of the subsidiary peaks closely determined by the energy differences between the 5^2P and the 4^2P states of rubidium and potassium, respectively.

ACKNOWLEDGMENTS

The authors are indebted to Dr. A. T. Forrester and R. C. Speiser for their encouragement and their contributions to the conception and development of the techniques. They also wish to thank Dr. D. G. Worden for criticisms and suggestions which aided in the interpretations of the results, and S. Snider for the construction and maintenance of the ever-changing apparatus.

[19] A. Salmona and M. J. Seaton, Proc. Phys. Soc. (London) **77**, 617 (1961).

[20] S. K. Allison, Rev. Mod. Phys. **30**, 1137 (1958).

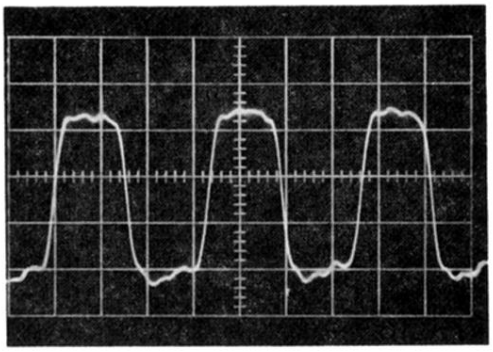

(a)

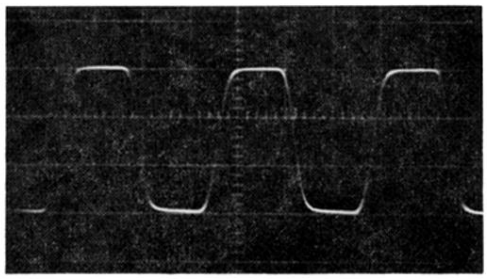

(b)

FIG. 4. Comparison of charge-transfer signal and atom-beam wave shapes from oscilloscope photos. Note the very favorable signal-to-noise ratio seen in the charge-transfer signal (peak-to-peak current of about 1.5×10^{-10} A). (a) Charge-transfer signal: Rb^{+}-Rb at 10 kV; vertical scale $=5\times10^{-11}$ A/div; horizontal scale = 10 ms/div. (b) Atom beam: Cs beam; ionizer temperature 992°C; vertical scale $=5\times10^{-6}$ A/div; horizontal scale = 10 ms/div.